

**Interpretation of Undrained
Self-Boring Pressuremeter Test
Results Incorporating Unloading**

by

R.S.Ferreira and P.K.Robertson

**Department of Civil Engineering
University of Alberta
Edmonton, Alberta
T6G 2G7 CANADA
Tel.(403) 492-5106**

**Canadian Geotechnical Journal
October 1991**

Interpretation of Undrained Self-Boring Pressuremeter Test Results Incorporating Unloading

Abstract

An interpretation method has been developed to incorporate nonlinear soil behaviour to interpret undrained pressuremeter test results. The method makes use of both the loading and unloading portions of the pressuremeter test. The proposed interpretation method accepts that some level of soil disturbance may exist during the early loading portion of the pressuremeter test. This is accomplished by putting greater emphasis on the unloading portion and the final part of the loading portion of the test. The method is evaluated using self-boring pressuremeter results from Fucino, Italy.

Keywords: Pressuremeter, interpretation, undrained, unloading

Introduction

The pressuremeter test has developed considerably since its first introduction by L. Menard in 1956. A number of publications have chronicled this development (Gambin, 1990; Baguelin et al, 1978; Wroth, 1984; Mair and Wood, 1987; Briaud and Consentino, 1990; Clough et al, 1990). Existing pressuremeter testing can be divided into two main groups: pre-bored and self-bored. The pre-bored pressuremeter test (PMT) is performed in a pre-drilled hole, whereas the self-bored pressuremeter test (SBPT) is self-bored into the soil in an effort to minimize soil disturbance. Recently, full-displacement pressuremeter tests (FDPT) have been developed (Hughes and Robertson, 1985; Withers et al, 1986; Campanella et al 1990) where the probe is pushed into the ground in a full-displacement manner. These different pressuremeter tests (PMT, SBPT and FDPT) are thought of as distinct and separate in situ testing techniques, with different interpretation methods. The PMT is usually analysed using empirical correlations related to specific design rules. The SBPT is generally performed in relatively soft soils and the results are analysed using theoretical relationships to derive basic soil parameters. The FDPT is relatively new and interpretation techniques are still evolving (Houlsby and Withers, 1988; Withers et al, 1989).

Most of the design rules based on the pre-bored pressuremeter originated from Menard's work in the early 1960's. The problem of soil disturbance is the most significant factor affecting PMT results. Investigations by Menard and the Laboratoire Central des Ponts et Chaussées (LCPC) in France have led to the development of standard procedures for Menard pre-bored pressuremeter tests. A complete description of these procedures are given in Baguelin et al (1978). The quality of foundation design using the Menard PMT is often very good, provided the tests are carried out according to the standard methods, using standard equipment in soils similar to those that have been studied in the development of the empirical design rules. In medium or stiff clays and soft rocks, where installation procedure is easier, and a good test hole can be formed, the results are usually more repeatable. However in soft saturated soils, soil disturbance can be significant and test results are not always repeatable. Full details of the various factors affecting PMT results are given by Baguelin et al (1978).

Efforts to minimize soil disturbance led to the development of self-boring pressuremeters in the early 1970's. This resulted in a series of developments related to the theoretical interpretation of the SBPT. However, the process of installation by current SBP's is not always efficient (Clough et al, 1990) and is often subject to problems, resulting in some disturbance especially in very stiff soils. Hence, most SBPT results are subject to some degree of disturbance, the level of disturbance tending to increase with increasing soil stiffness. Soil disturbance during installation of the SBP has the greatest effect on the shape of the initial loading portion of the pressuremeter curve. It is therefore, common practice to put less reliance on the initial loading portion of SBPT results. This philosophy has also been incorporated into many of the Menard design rules, where greater reliance is often placed on the limit pressure (P_L) at large strains rather than the pressuremeter modulus (E_M) which is known to be sensitive to soil disturbance.

The introduction of the SBPT has resulted in substantial research related to various theoretical interpretation techniques of the SBPT results to give basic soil parameters. Almost all of these developments have resulted in interpretation techniques that utilize only the loading portion of the SBPT. Recently, Jefferies (1988) proposed that the interpretation of undrained SBPT results in clay could be extended to include the unloading part of the test. Housby and Withers (1988) also incorporated the unloading portion for interpretation of FDPT results in clay. Both Jefferies (1988) and Housby and Withers (1988) methods utilize simple elastic-perfectly plastic soil models. Several studies (Hughes and Robertson, 1985; Robertson, 1982; Robertson and Hughes, 1986; Bellotti et al 1986; Schnaid and Housby, 1990) have shown that the unloading portion of pressuremeter tests appear to be insensitive to disturbance caused due to installation. It would, therefore, appear useful and logical to incorporate the unloading portion of pressuremeter tests into any interpretation technique.

The main objective of this paper is to describe an extension of the work by Jefferies (1988) to incorporate nonlinear soil behaviour to interpret undrained SBPT results. The interpretation makes use of both the loading and unloading portions of the test. An interpretation methodology is described and illustrated with SBPT data from a site in Italy. The interpretation methodology developed does not require

SBPT data with perfect self-boring installation since much of the emphasis is placed on the unloading portion of the test.

Interpretation of undrained pressuremeter results

One of the earliest pressuremeter interpretation methods was developed by Gibson and Anderson (1961) to define a limit pressure for pressuremeter expansion in an ideal elastic-perfectly plastic material. Commonly, the pressuremeter results are plotted in terms of radial pressure (σ_r) versus $\log_e(\Delta V/V)$, where $(\Delta V/V)$ is a measurement of the cavity strain related to the deformed state. The results of the plastic phase of the test should lie on a straight line with a gradient equal to the undrained shear strength (S_u). The method is still very popular for interpreting pressuremeter tests (both PMT and SBPT's) in clay, partly due to its reliance on the large strain (plastic) portion of the test which is less affected by soil disturbance.

In 1972, analytical solutions (Palmer, 1972; Ladanyi, 1972; Baguelin et al, 1972) were developed that allowed the complete undrained stress-strain curve of the soil to be derived from SBPT results of an undrained test. The solution uses the slope of the pressuremeter loading curve and assumes the soil to have a unique, but not pre-defined stress-strain relationship. Experience gained with this approach showed that in many cases the derived stress-strain curve has an irregular shape due to the difficulty in obtaining the slope of the pressure-expansion curve. Therefore, several methods were developed (Jamiolkowski and Lancellotta, 1977a, 1977b; Denby, 1978; Arnold, 1981) to smooth the measured pressure-expansion curve using different curve fitting techniques. All these techniques were developed to interpret the loading portion of the pressuremeter test. Hence, any soil disturbance caused by installation was reflected in some unknown manner in the interpreted results.

Houlsby and Withers (1988) suggested that full-displacement pressuremeter tests in clay could be analysed using the unloading portion of the test results. The soil was assumed to be elastic-perfectly plastic, principal stress rotation due to unloading was assumed to occur when reverse plasticity takes place and a large strain analysis was applied. A closed-form solution was developed and the undrained shear strength is determined from a geometric

construction using the unloading curve, somewhat similar to the subtangent construction used in the Palmer (1972) method. This method represents the first attempt to obtain information on soil parameters using the complete unloading portion of a pressuremeter test.

Jefferies (1988) proposed a method to interpret SBPT results in clay incorporating the complete loading and unloading portion of the test. The method was also based on an elastic-perfectly plastic soil model. The ratio of the unloading strength of the clay to the loading strength was assumed to be known. Jefferies' method assumed that the installation was carried out with minimum disturbance (i.e. perfect self-boring process) so that the loading portion of the test represented the true undisturbed response of the soil. Jefferies (1988) used computer aided modelling techniques to visually compare the measured response with the numerically derived curves. The method required specialized interactive software operating on an engineering workstation (or microcomputer with high resolution screen monitor). The primary objective of the method was to derive the in situ horizontal stress, although the undrained shear strength (S_u) and an equivalent linear elastic shear modulus (G) was also derived. The Jefferies' approach represents one of the first attempts to use all of the information contained in the loading and unloading portions of a SBPT to derive the required soil parameters. However, the technique required specialized interactive software and perfect SBPT results. Also the simplified elastic-perfectly plastic soil model made it difficult to understand the meaning of the equivalent linear elastic shear modulus for application to design problems.

Proposed method

The proposed method is an extension of the method developed by Jefferies (1988). However, soil nonlinearity is incorporated assuming the soil stress-strain response can be represented by a hyperbolic function. The method has the following assumptions:

- (1) The pressuremeter test is performed undrained from the start of expansion to complete contraction;
- (2) The test is treated as an expansion of an infinity long cylindrical cavity (i.e. radially symmetric plane strain);
- (3) The vertical stress remains the intermediate principal stress;

- (4) The soil stress-strain behaviour can be represented by a hyperbolic function in both loading and unloading;
- (5) The ratio of the unloading strength of the clay to the loading strength is known;
- (6) Strains are considered to be small.

These assumptions are essentially the same as those made by Jefferies (1988) and Gibson and Anderson (1961), except for the hyperbolic representation of the stress-strain behaviour. The selection of the hyperbolic representation of soil behaviour was made for the following reasons:

- (1) The hyperbolic stress-strain model (Kondner, 1963) has proven effective in describing soil behaviour under a variety of loading conditions (Duncan and Chang, 1970);
- (2) The need to keep the soil model simple and to avoid generating a method that requires a solution for many unknown parameters;
- (3) The parameters that define the soil model have some engineering significance, so that when the interpretation process is completed the parameters derived can be understood and applied in design.

For pressuremeter testing the circumferential strain (ϵ_0) is often referred as the cavity strain (ϵ). For pressuremeter expansion, the cavity strain is defined as:

$$\epsilon = \frac{\Delta R}{R_0} \text{-----}(1)$$

where: R_0 - initial radius of the pressuremeter
 ΔR - change in pressuremeter radius ($\Delta R = R - R_0$)
 R - current radius of the pressuremeter

For pressuremeter contraction, the cavity strain is defined as:

$$\epsilon^* = \frac{\Delta R}{R_{\max}} \text{-----}(2)$$

where: R_{\max} - maximum radius of the pressuremeter
 ΔR - change in pressuremeter radius ($\Delta R = R - R_{\max}$)
 R - current radius of the pressuremeter

The hyperbolic model for loading is defined in terms of the shear stress (τ) and the cavity strain (ϵ) as follows:

$$\tau = \frac{\epsilon}{\frac{1}{2G_i} + \frac{\epsilon}{\tau_{uh}}} \text{-----}(3)$$

where: τ - mobilized shear stress
 G_i - initial shear modulus
 τ_{uh} - ultimate undrained shear strength during loading
 ϵ - cavity strain at the pressuremeter wall (loading)

The hyperbolic model is usually applied in terms of shear stress (τ) and shear strain (γ). However, for undrained cylindrical cavity expansion the following relationship holds:

$$\gamma = 2\epsilon \text{-----}(4)$$

Hence, the term $2G_i$ in equation (3) stems from the use of cavity strain (ϵ) instead of the more conventional engineering shear strain (γ).

The complete stress-strain curve of the soil can then be defined using equation (3) and the two parameters G_i and τ_{uh} . The parameter G_i represents the initial tangent shear modulus at small strains. The level of strain that G_i is applicable is dependent on the strain range over which the hyperbolic function adequately fits the stress-strain response of the soil. Recent research would suggest that G_i is applicable from a shear strain level of approximately 0.1%.

The hyperbolic model for unloading is defined as follows:

$$\tau^* = \frac{\epsilon^*}{\frac{1}{2G_i} - \frac{\epsilon^*}{\tau_{uh}^*}} \text{-----}(5)$$

where: τ^* - mobilized shear stress

- ϵ^* - cavity strain at the pressuremeter wall (unloading)
 τ_{uh}^* - ultimate undrained shear strength during unloading

The resulting loading and unloading model is illustrated in figure 1. The hyperbolic soil model when combined with the governing equations of equilibrium of stresses, compatibility of strains and the boundary conditions for a pressuremeter produce the following closed form solutions:

(a) loading

$$p = \sigma_{h_0} + \frac{\tau_{uh}^*}{R_\tau} \cdot \ln \left(1 + \frac{2G_i \cdot R_\tau \cdot \epsilon}{\tau_{uh}^*} \right) \text{-----}(6)$$

(b) unloading

$$p = p_{\max} + \tau_{uh}^* \cdot \ln \left(\frac{1}{1 - \frac{2G_i \cdot (\epsilon - \epsilon_{\max})}{(1 + \epsilon_{\max}) \cdot \tau_{uh}^*}} \right) \text{-----}(7)$$

- where: p - pressuremeter expansion or contraction pressure exerted on soil after correction for membrane stiffness
- σ_{h_0} - initial horizontal in situ stress
- $R_\tau = \tau_{uh}^* / \tau_{uh}$ - ratio of ultimate undrained shear strength on unloading and loading
- ϵ_{\max} - cavity strain at the cavity (pressuremeter) wall at beginning of unloading
- p_{\max} - pressure at the cavity wall at beginning of unloading

The loading and unloading parts of the pressuremeter test can be fitted using equations (6) and (7), respectively, to derive the parameters G_i , τ_{uh} and σ_{h_0} . Full details of the derivations are given in an appendix to this paper.

Proposed methodology

As discussed earlier, the unloading part of the pressuremeter curve is less influenced by disturbance during installation. Hence, it is logical to first analyse the unloading part of the test to derive τ_{uh}^* and G_i . If a value for the ratio R_τ is assumed, the undrained shear strength in loading (τ_{uh}) is therefore determined. Using these values of τ_{uh}^* , G_i and R_τ the loading part of the test can then be analysed to derive σ_{h_0} .

If the loading part of the test is influenced by disturbance, the early part of the loading portion will not agree with the derived curve. Hence, the loading part of the test should only be analysed over the last part of the curve, which will, in general be less influenced by disturbance. Based on this logic, the following steps are prescribed for the proposed interpretation methodology.

- (a) Use the unloading analytical equation (7) to fit the unloading portion of the pressuremeter test. Two parameters are derived from the best fit: τ_{uh}^* and G_i .
- (b) Assume a value for $R_\tau (= \tau_{uh}^*/\tau_{uh})$ and apply the derived values of τ_{uh}^* and G_i to fit the last part of the loading portion of the pressuremeter test to determine σ_{h_0} .

This interpretation methodology is shown schematically in figure 2.

This process accepts that the initial loading portion of the pressuremeter test is influenced by some amount of disturbance. If the self-boring installation process has resulted in very little disturbance the analytical curve should match closely the entire measured pressuremeter curve.

This methodology also allows this procedure to be applied to undrained pre-bored pressuremeter (PMT) and full-displacement (cone-) pressuremeter (FDPT) test results.

Figure 3 illustrates schematically how this concept can be applied to PMT and FDPT results. Its application to PMT and FDPT results requires the assumption that the final point of the loading curve represents failure of a significant mass of undisturbed soil. During initial loading the pressuremeter response is controlled mostly by the disturbed soil adjacent to the probe. However, as pressuremeter expansion continues, the zone of soil taken to failure continues to grow outwards from the probe. If the pressuremeter is expanded sufficiently large, the pressuremeter response will be dominated by undisturbed soil.

The proposed method (equations 6 and 7) is based on small strains and would not be applicable to large strain pressuremeter expansion. A large strain solution is currently under development and will be evaluated shortly in a subsequent publication.

Ratio of undrained strength in loading and unloading (R_τ)

As presented in the interpretation methodology, the parameter R_τ is required to obtain the value of the undrained shear strength τ_{uh} and the horizontal in situ initial stress, σ_{hs} . Ideally, the parameter R_τ should be obtained from laboratory testing on high quality undisturbed samples, tested under stress paths similar to those experienced during undrained pressuremeter expansion and contraction, as suggested by Jefferies (1988). However, for the initial interpretation of most pressuremeter tests this is not possible, and an estimate of R_τ should be made.

Undrained pressuremeter expansion and contraction can be considered to be a plain strain problem where the stress path in unloading is the reverse of loading. Hence, since the plane strain strength envelope is the same in loading and unloading, it is reasonable to assume that $R_\tau = 2.0$. Both Jefferies (1988) and Houlsby and Withers (1988) also assumed that the strength in loading equals the strength in unloading. Therefore, for the soil model used in this methodology the value of the ratio R_τ is assumed to be 2.0.

Application examples

The proposed methodology has been applied to high quality SBPT results performed in a uniform clay deposit, reported by Fioravante(1988) and A.G.I.-Associazione Geotecnica Italiana (1991).

Software to perform curve fitting

Several approaches can be used to fit an equation to experimental data. Rather than develop specific software to perform the curve fitting process using an optimization routine, it is preferable to use available application software developed for personal computers. The software selected for this study was Kaleidagraph™ (version 2.1) developed for a Macintosh™ microcomputer. This application is a powerful tool to perform calculations, graphs and curve fitting.

The experimental data, from the field, after being corrected for membrane stiffness, is copied to a Kaleidagraph™ worksheet, so the data becomes available for analyses. The only manipulation needed is to separate the loading and unloading portions of the test, eliminate any unload-reload loop data, and arrange both sets of remaining data in ascending order. The data are then ready to be analysed.

The least square error curve fitting method was used to fit a general function to a set of experimental data. This is a very simple and well understood method and can be used readily when the data does not present a large scatter and has a defined trend. This is the case of the data from pressuremeter tests.

Loading and unloading analytical equations are entered and the curve fitting is performed. As a result, a graph is automatically displayed on the monitor screen, and a visual check of the match between the experimental and analytical curves can be made. It is noteworthy to mention at this point, that the first set of parameter values to be tested, must be given by the user. For fitting the unloading curve the only requirement for this first guess is that the parameters should have the same order of magnitude as the set which will give the best curve fitting. Hence, one can avoid divergence of the analysis. However, for fitting the loading curve the first guess must consider: (a) minimum number of experimental points used; and (b) minimum range of pressure for those points. Experience with this software has shown that the number of points

must be greater than 15 and the range of pressure must be sufficient to obtain a correlation factor between 0 and 1.0. The reader is referred to the Kaleidagraph™ manual for more information on using the application and curve fitting capabilities.

A suggested interpretation template is presented in figure 4.

Interpretation of tests in Fucino clay

Fioravante (1988) presented 36 self-boring pressuremeter test results performed in Fucino Clay in two boreholes, at the same site. A complete geotechnical characterization of the Fucino clay is presented by AGI (1991). The clay deposit, located within the central Apennines, is described as a soft, homogeneous, highly structured CaCO_3 cemented, lacustrine clay. The cementation with calcium carbonate plays an important role in the mechanical behaviour of the clay, being responsible for some discrepancies shown by different tests, mainly when disturbance is present.

From the SBPT results presented by Fioravante (1988), 20 tests from borehole two, have been interpreted and the results presented. The first test is 2m deep and the last one is 38m deep. All tests are interpreted using the methodology described earlier. As an example, figure 5 presents the interpretation of the test V2P14 (depth 26m) including two typical graphs. The template shown in figure 4 also includes the interpretation of test V2P14.

Test V2P14 appears to represent a good SBPT with little disturbance. Figure 5b shows that the analytical solution with $R_t = 2.0$ provides an excellent fit to all the measured loading curve. For the final interpretation, shown on figure 5a, only the very last points of the loading curve have been chosen to apply the curve fitting technique. The good agreement between the fit to all the data points and the fit to only the last points implies the test has suffered little disturbance due to the installation process. Figure 4 illustrates the suggested process towards full interpretation.

Figure 6 presents the interpretation for test V2P10 (depth 18m). This test appears to have some disturbance, since the analytical solution does not provide a good match to the complete loading curve. Note that the solution shown in figure 6 was obtained by matching only the final portion of the loading curve. When the fit

was performed over the complete loading curve, the match was poor over the last part of the experimental curve.

Initial shear modulus (G_i)

The interpreted initial shear modulus values for all twenty tests are presented in figure 7. The interpreted values of G_i are very close to the shear modulus values calculated from unload-reload loops presented by AGI (1991), and approximately one third the values determined from in situ shear wave velocity measurements.

The shear modulus (G_0) determined from in situ shear wave velocity measurements represents the elastic shear modulus at a strain level of less than $10^{-4}\%$. The unload-reload modulus (G_{ur}) represents the average modulus over an average shear strain level of $10^{-1}\%$ (Robertson, 1982; Bellotti et al 1986). The interpreted shear modulus (G_i) derived from the proposed interpretation is based on an assumed hyperbolic stress-strain relationship. Experience has shown that the hyperbolic expression is a reasonable representation of the stress-strain response of many soils over a variety of strain ranges (Vucetic and Dobry, 1991). Hardin and Drnevich (1972a, 1972b) suggested that the hyperbolic expression could represent the stress-strain response of many soils from the very small shear strain of $10^{-4}\%$ to about $10^{-1}\%$. However, Duncan and Chang (1970) showed that the hyperbolic expression was very good to describe the stress-strain response from an initial shear strain of around $10^{-1}\%$ to failure ($>1\%$).

The results shown in figure 7 suggest that the hyperbolic expression is a reasonable representation of the stress-strain response from around $10^{-1}\%$ to failure for Fucino clay.

Undrained shear strength (τ_{sk})

When using the hyperbolic relationship to describe the nonlinear stress-strain behaviour of soil, the ultimate shear stress or undrained shear strength is only reached at infinite strain. Traditionally this has been overcome by incorporating a reduction factor (R_f) to allow the undrained shear strength to be attained at a known strain level.

However, if a reduction factor is incorporated into the proposed interpretation method, the following problems occur:

- (1) Additional parameter is needed to define the reduction factor (R_f);
- (2) Closed form solution is difficult to obtain because of the discontinuity in the stress-strain curve due to the reduction factor cut-off.

Although the ultimate shear stress is not attained in the hyperbolic representation, it is possible to calculate the mobilized undrained shear stress ($S_{u|_{mob}}$) reached at the strain level in the pressuremeter test. Figure 8 shows the interpreted range for the mobilized pressuremeter undrained shear stress ($S_{u|_{mob}}$) for the Fucino clay compared to undrained shear strength from field vane, flat dilatometer and laboratory undrained triaxial tests (UU). Also shown are the undrained shear strengths derived from SBPT results using only the loading portion of the pressuremeter test. The results are in good agreement at a depth around 5m. At a depth greater than 5m the interpreted values using the SBPT results are significantly higher than the other tests. High undrained shear strengths from pressuremeter tests has been frequently observed. Wroth (1984) showed that the undrained shear strength derived from a SBPT should be larger than the strength derived from a field vane test due to the different stress paths followed. Wroth (1984) suggested that the SBPT S_u values should be larger than the field vane by about 40% depending on the friction angle of the clay. If the SBPT S_u values in figure 8 are corrected based on the suggestion by Wroth (1984), the SBPT S_u values would remain larger than the field vane values.

It has been recognized by many researchers (Wroth 1984; Anderson and Pyrah 1986; Williams 1986) that some drainage and creep takes place during many pressuremeter tests in clay. This drainage and creep can result in overestimated undrained shear strength. Partial drainage and strain rate effects (creep) are common problems when interpreting in situ tests in fine grained soils.

Earth pressure coefficient at rest (K_0)

Figure 9 shows the interpreted values for the earth pressure coefficient at rest using the proposed methodology, compared to values determined from flat dilatometer tests and from the observed lift-off pressure of self-boring pressuremeter tests. In general, the interpreted values of K_0 using the proposed interpretation methodology are slightly higher than the values obtained from the lift-off pressure.

Wroth(1975) stated that it is impossible to measure the in situ stress at rest with any device which depends upon of the insertion of any type of instrument into the soil mass. However, providing a careful insertion, and minimum disturbance, it has been recognized that the self-boring pressuremeter data should carry useful information on the initial horizontal stress. For a pre-defined value for ratio R_c it appears possible to derive acceptable values for σ_h , using the proposed interpretation method even if the loading curve has been somewhat influenced by disturbance during installation. This pre-defined value for the ratio R_c can be assumed to be 2.0 or determined from laboratory tests, as proposed by Jefferies (1988).

Sensitivity of interpretation

To illustrate the sensitivity of the proposed interpretation method, test V2P14 has been reanalysed varying one of the variables by $\pm 10\%$ of the interpreted value. The parameters selected were those derived (figure 4) to provide the best fit using the proposed methodology.

Figure 10 presents the variation in analytical loading curve for a $\pm 10\%$ change in τ_{ult} . The initial horizontal stress and shear modulus values were maintained constant. It is evident from figure 10 that a small change in the ultimate shear strength has an influence on the size of the loading curve. Although the influence is not dramatic, a noticeable change is evident in the value of the maximum pressure.

Figure 11 presents the variation in analytical loading curve for a $\pm 10\%$ change in G_i . The initial horizontal stress and the undrained shear strength were maintained constant. Figure 11 shows that a

small change in shear modulus has little influence on the final analytical loading curve.

Figure 12 presents the variation in analytical loading curve for a $\pm 10\%$ change in σ_{ho} . The shear modulus and undrained shear strength were maintained constant. Figure 12 shows that a small change in horizontal stress results in a large change in the analytical loading curve. The initial horizontal stress is, therefore an important parameter of this method. Hence, it should be possible to evaluate in-situ stress to high degree of accuracy using curve fitting techniques.

Conclusions

A method to interpret undrained pressuremeter results in clay has been presented. The method incorporates the unloading portion of the pressuremeter test to derive the initial shear modulus and undrained shear strength. The soil response is represented by a hyperbolic relationship between the shear stress and circumferential strain. The method accepts that some level of disturbance may exist for self-boring pressuremeter test results and hence, only the later part of the loading curve is used to derive the in situ stress.

Pre-bored and full-displacement undrained pressuremeter test results can also be analysed using the proposed method provided the loading portion of the test has been taken sufficient volume of undisturbed soil to failure. This may require large expansion in some soils. The current method is based on small strains and will therefore not apply to large pressuremeter expansions. A subsequent paper will present a large strain nonlinear solution and illustrate how this can be applied to pre-bored and full-displacement pressuremeter tests.

To apply the proposed interpretation methodology a value for the ratio of the undrained shear strength in unloading and loading (R_t) must be known. A value of 2.0 is recommended. To improve the interpretation of in-situ stress and undrained shear strength the ratio of undrained shear strength in unloading and loading (R_t) should be measured on undisturbed samples following stress paths similar to those in the pressuremeter test.

The proposed interpretation method involves comparison of the measured loading and unloading pressuremeter curves with analytically derived curves. This comparison can be achieved using commercially available microcomputer application software. For this study the software was Kaleidagraph™ (version 2.1) developed and operated for the Macintosh™ microcomputer. Hence, it should be possible for practicing engineers to apply this proposed method to SBPT results without the need of special customized software.

The proposed interpretation method has been evaluated using 20 high quality self-boring pressuremeter results performed in Fucino clay in Italy. The interpreted soil parameters had reasonable values when compared to other in situ and laboratory test results.

The proposed interpretation method presents an acceptable framework to derive soil parameters from undrained pressuremeter tests in fine grained soils. This framework involves the complete loading and unloading portions of the test and incorporates nonlinearity of the soil response in a simple closed-form manner.

Acknowledgements

This research was possible due to the permission granted from the Federal University of Santa Catarina - Brazil, to the first author to do his Ph.D. studies at the University of Alberta, during the period from August/88 to July/92. The scholarship received from the Brazilian Government, through CAPES-MEC is also gratefully acknowledged. The authors would also like to acknowledge Prof. M. Jamiolkowski for providing the pressuremeter data for Fucino clay.

Special consideration is due to Mss. Claudia Dutra Ferreira, whose attention and expertise in typing the manuscripts are sincerely appreciated.

Appendix

Derivation of the pressuremeter analytical equation

Strain definition and signal convention

Compressive strains and stresses are positive.

For pressuremeter expansion, the cavity strain is defined as:

$$\epsilon = \frac{\Delta R}{R_0} \text{-----(A1)}$$

where: R_0 - initial radius of the pressuremeter
 ΔR - change in pressuremeter radius ($\Delta R = R - R_0$)
 R - current radius of the pressuremeter

For pressuremeter contraction, the cavity strain is defined as:

$$\epsilon^* = \frac{\Delta R}{R_{\max}} \text{-----(A2)}$$

where: R_{\max} - maximum radius of the pressuremeter
 ΔR - change in pressuremeter radius ($\Delta R = R - R_{\max}$)
 R - current radius of the pressuremeter

Governing equations

(1) Baguelin(1972), Palmer(1972), Ladanyi(1972)

$$\frac{d\sigma_r}{d\epsilon} = \frac{2\tau(\epsilon)}{\epsilon(2+\epsilon)(1+\epsilon)} \text{-----(A3)}$$

where: σ_r - radial stress applied to the soil element
 $\tau(\epsilon)$ - constitutive relationship

For small strains the equation reduces to:

$$\frac{d\sigma_r}{d\epsilon} = \frac{\tau(\epsilon)}{\epsilon} \text{-----(A4)}$$

(2) Constitutive relationship (hyperbolic model)

(a) Loading:

$$\tau = \frac{\varepsilon}{\frac{1}{2G_i} + \frac{\varepsilon}{\tau_{uk}}} \text{-----(A5)}$$

where: τ - mobilized shear strain
 $2G_i$ - initial shear modulus
 τ_{uk} - ultimate shear strength (asymptote)

(b) Unloading:

$$\tau^* = \frac{\varepsilon^*}{\frac{1}{2G_i} - \frac{\varepsilon^*}{\tau_{uk}^*}} \text{-----(A6)}$$

where: τ^* - mobilized shear strength
 ε^* - circumferential strain (negative under unloading)
 τ_{uk}^* - ultimate shear strength (asymptote)

C. Boundary conditions at the cavity wall

(a) Loading:

$$\varepsilon = 0 \Rightarrow \sigma_r = \sigma_{h_0} \text{-----(A7)}$$

(b) Unloading:

$$\varepsilon^* = 0 \Rightarrow \sigma_r = \sigma_{\max} \text{-----(A8)}$$

D. Pressuremeter analytical equation

(a) Loading:

$$p = \sigma_{h_0} + \frac{\tau_{uk}^*}{R_c} \cdot \ln \left(1 + \frac{2G_i \cdot R_c \cdot \varepsilon}{\tau_{uk}^*} \right) \text{-----(A9)}$$

valid for $0 \leq \varepsilon \leq \varepsilon_{L|\max}$

- where: $p \equiv \sigma_r$ - pressure at the cavity wall at beginning of unloading
 σ_{h_0} - initial horizontal stress
 $R_\tau = \tau_{uk}^* / \tau_{uk}$ - ratio of ultimate undrained shear strength on unloading and loading
 $\varepsilon_{L|_{\max}}$ - cavity strain wall at the end of loading

(b) Unloading:

$$p = p_{\max} + \tau_{uk}^* \cdot \ln \left(\frac{1}{1 - \frac{2G_i \cdot (\varepsilon - \varepsilon_{\max})}{(1 + \varepsilon_{\max}) \cdot \tau_{uk}^*}} \right) \text{----- (A10)}$$

valid for $0 \geq \varepsilon^* \geq -\varepsilon_{\max}$

- where: $p_{\max} \equiv \sigma_r|_{\max}$ - pressure at the cavity wall at beginning of unloading

$$\varepsilon^* = \frac{\varepsilon - \varepsilon_{\max}}{1 + \varepsilon_{\max}} \text{----- (A11)}$$

- where: ε_{\max} - cavity strain at the beginning of unloading

Notation

(1) Latin symbols

- E_M - pressuremeter modulus
 G - elastic shear modulus
 G_i - initial elastic shear modulus (hyperbolic model)
 G_{ur} - shear modulus from unload-reload loops
 G_0 - small strain shear modulus from in situ shear wave velocities
 \log_e and \ln - natural logarithm

p	- pressure at the cavity wall
P_L	- limit pressure
p_{\max}	- pressure at the cavity wall at beginning of unloading
R	- current pressuremeter radius
R_f	- reduction factor of hyperbolic model
R_{\max}	- maximum radius of the pressuremeter
R_τ	- ratio of ultimate undrained shear strength on unloading and loading
R_0	- initial radius of the pressuremeter
r	- radial coordinate
S_u	- undrained shear strength
$S_u _{\text{mob}}$	- mobilized undrained shear strength

(2) Greek symbols

γ	- engineering shear strain
ΔR	- change in pressuremeter radius
$\Delta V/V$	- volumetric cavity strain
ϵ	- cavity strain in loading
ϵ_{\max}	- cavity strain at the beginning of unloading
$\epsilon_L _{\max}$	- cavity strain at the end of loading
ϵ^*	- cavity strain in unloading
ϵ_θ	- circumferential strain
σ_r	- radial stress
σ_{h_0}	- initial horizontal in-situ stress
τ	- mobilized shear stress in loading
τ_{uL}	- ultimate undrained shear strength in loading
τ^*	- mobilized shear stress in unloading
τ_{uL}^*	- ultimate shear strength in unloading
$\tau(\epsilon)$	- shear stress-circumferential strain relationship

Acronyms

AGI	- Associazione Geotecnica Italiana
FDPT	- Full-displacement pressuremeter test
LCPC	- Laboratoire Central des Ponts et Chaussées
OCR	- Overconsolidation ratio
SBP	- Self-boring pressuremeter
SBPT	- Self-boring pressuremeter test

References

1. AGI 1991. Geotechnical characterization of Fucino clay
X European Conference on Soil Mechanics and Foundation Engineering, ???: pp ???Firenze - Italy.
2. Anderson, W.F., and Pyrah, I.C. 1986. Undrained strength and deformation parameters from pressuremeter test results. The Pressuremeter and Its Marine Applications : Second International Symposium, pp.324-338.
3. Arnold, M. 1981. An empirical evaluation of pressuremeter test data. Canadian Geotechnical Journal, 18: pp.455-459.
4. Baguelin, F., Jezequel, J.F., and Shields, D.H. 1978. The Pressuremeter and Foundation Engineering. Trans Tech Publications.
5. Baguelin, F., Jezequel, J.F., Mee, E.L., and Mehaute, A.L. 1972. Expansion of cylindrical probes in cohesive soils. ASCE - Journal of the Soil Mechanics and Foundations Division, 98: pp.1129-1142.
6. Bellotti, R., Ghionna, V., Jamiolkowski, M., Lancellotta, R., and Manfredini, G. 1986. Deformation characteristics of cohesionless soils from in situ tests. In Situ '86 - Use of In Situ Tests in Geotechnical Engineering, ASCE, Blacksburg, pp.47-73.
7. Briaud, J.L., and Cosentino, P.J. 1990. Pavement design with the pavement pressuremeter. Proceedings of the Third International Symposium on Pressuremeters, Oxford, pp.401-413
8. Campanella, R.G., Howie, J.A., Sully, J.P., and Robertson, P.K. 1990. Evaluation of cone pressuremeter tests in soft cohesive soils. Proceedings of the Third International Symposium on Pressuremeters, Oxford, pp.125-135.
9. Clough, G.W., Briaud, J.L., and Hughes, J.M.O. 1990. The development of pressuremeter testing. Proceedings of the Third International Symposium on Pressuremeters, Oxford, pp.25-45.
10. Denby, G.M. 1978. Self-boring pressuremeter study of the San Francisco Bay mud. Ph.D. Thesis, Stanford University.

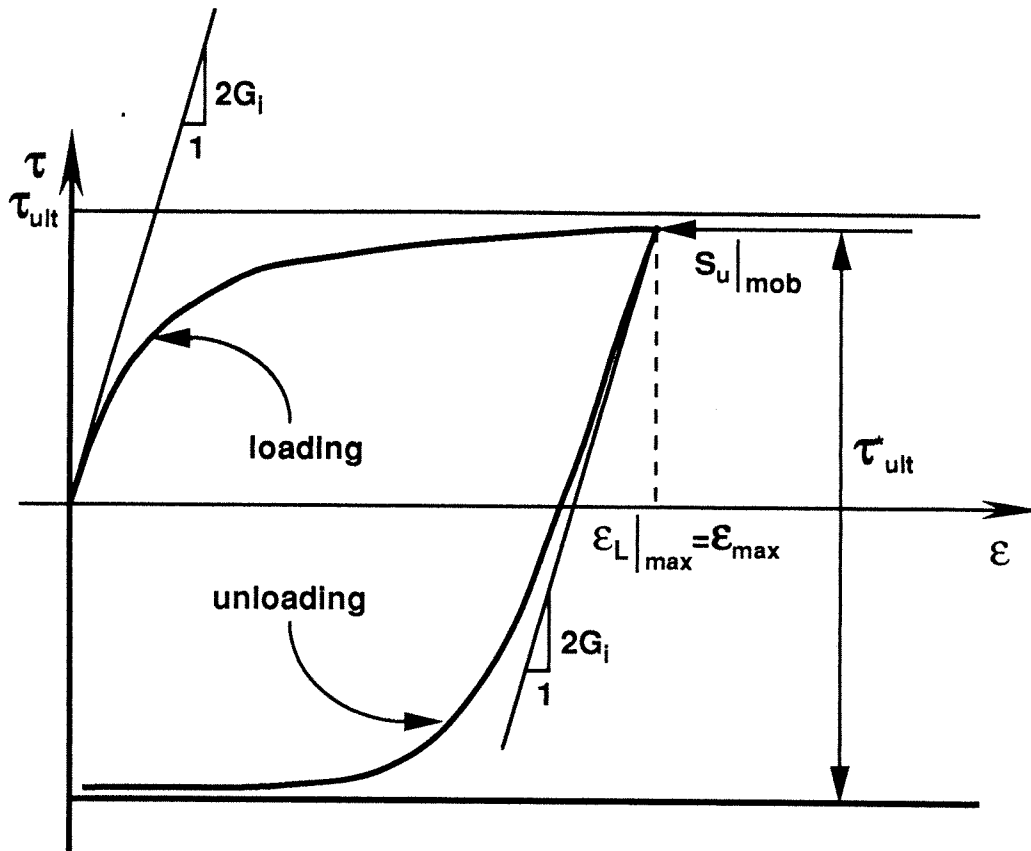
11. Duncan, J.M., and Chang, C.Y. 1970. Nonlinear analysis of stress and strain in soils. *Journal of the Soil Mechanics and Foundation Division, ASCE*, 96: SM5, pp.1629-1653.
12. Fioravante, V. 1988. Interpretazione delle prove pressiometriche in argille con particolare riferimento alla fase di holding. Dottorato di Ricerca in Ingegneria Geotecnica. Politecnico di Torino. Italy
13. Gambin, M.P. 1990. The history of pressuremeter practice in France. *Proceedings of the Third International Symposium on Pressuremeters*, Oxford, pp.5-24.
14. Gibson, R.E., and Anderson, W.F. 1961. In situ measurement of soil properties with the pressuremeter. *Civil Engineering and Public Works Review*, 56: pp.615-618.
15. Hardin, B.O., and Drnevich, V.P. 1972a. Shear modulus and damping in soils: Measurements and parameters effects. *Journal of the Soil Mechanics and Foundation Division, ASCE* , 98: pp.603-624.
16. Hardin, B.O., and Drnevich, V.P. 1972b. Shear modulus and damping in soils: Design equations and curves. *Journal of the Soil Mechanics and Foundation Division, ASCE* , 98: pp.667-692.
17. Houlsby, G.T., and Withers, N.J. 1988. Analysis of the cone-pressuremeter test in clay. *Géotechnique*, 38: N°4, pp.575-587.
18. Hughes, J.M.O., and Robertson, P.K. 1985. Full displacement pressuremeter testing in sands. *Canadian Geotechnical Journal*, 22: No.3, pp.???
19. Jamiolkowski, M., and Lancellotta, R. 1977a. Remarks on the use of self-boring pressuremeter in three Italian clays. *Revista Italiana Geotecnica*, 11: No.3.
20. Jamiolkowski, M., and Lancellotta, R. 1977b. On the reliability of the strength and and deformation characteristics as deduced from the self-boring pressuremeter tests. IX I.C.S.M.F.E. Tokyo, Discussion.
21. Jefferies, M.G. 1988. Determination of horizontal geostatic stress in clay with self-bored pressuremeter. *Canadian Geotechnical Journal*, 25: pp.559-573.

22. Kondner, R.L. 1963. Hyperbolic stress-strain response : cohesive soil. *Journal of the Soil Mechanics and Foundation Division, ASCE*, 89: pp.115-143.
23. Ladanyi, B. 1972. In situ determination of undrained stress-strain behaviour of sensitive clays with the pressuremeter. *Canadian Geotechnical Journal*, 9: pp.313-319.
24. Mair, R.J., and Wood, D.M. 1987. Pressuremeter testing - Methods and interpretation. CIRIA Ground Engineering Report : In situ testing - Butterworths, pp.160.
25. Palmer, A.C. 1972. Undrained plane-strain expansion of a cylindrical cavity in clay: a simple interpretation of the pressuremeter test. *Géotechnique*, 22: pp.451-457.
26. Robertson, P.K. 1982. In situ testing of soil with emphasis on its application to liquefaction assessment. Ph.D. University of British Columbia, Vancouver.
27. Robertson, P.K., and Hughes, J.M.O. 1986. Determination of properties of sand from self-boring pressuremeter tests. *The pressuremeter and Its Marine Applications : Second International Symposium*, pp.283-302.
28. Schnaid, F., and Houlsby, G.T. 1990. Calibration chamber tests of the cone pressuremeter in sand. *Proceedings of the Third International Symposium on Pressuremeters*, Oxford, pp.263-272.
29. Vucetic, M., and Dobry, R. 1991. Effect of soil plasticity on cyclic response. *Journal of the Geotechnical Engineering Division, ASCE*, 117: pp.89-107.
30. Williams, D.J. 1986. Evaluation of different soil tests for determining design parameters. *Interpretation of Field Testing for Design Parameters*, Adelaide, pp.174-179.
31. Withers, N.J., Schaap, L.H.J., and Dalton, C.P. 1986. The development of a full displacement pressuremeter. *The Pressuremeter and Its Marine Applications : Second International Symposium*, pp.38-56.

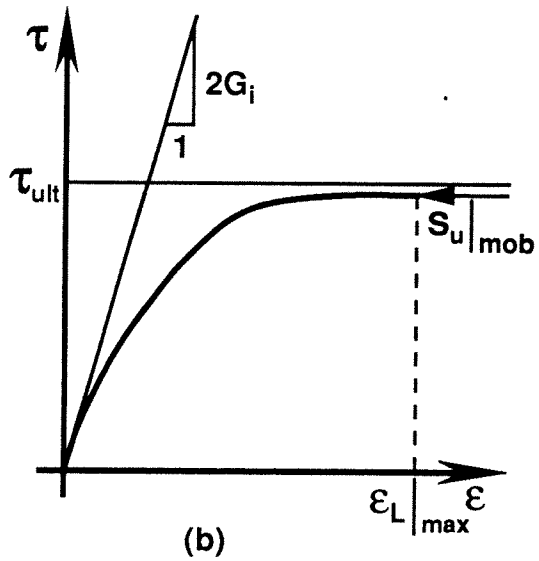
32. Withers, N.J., Howie, J., Hughes, J.M.O., and Robertson, P.K. 1989. Performance and analysis of cone pressuremeter tests in sands. *Géotechnique*, 39: N°3, pp.433-454.
33. Wroth, C.P. 1984. The interpretation of in situ soil tests. *Géotechnique*, 34: pp.449-489.
34. Wroth, C.P. 1975. In Situ Measurement of initial stresses and deformation characteristics. Proceedings of the Conference on In situ Measurement of Soil Properties, Raleigh, 2: pp.181-230.

List of figures

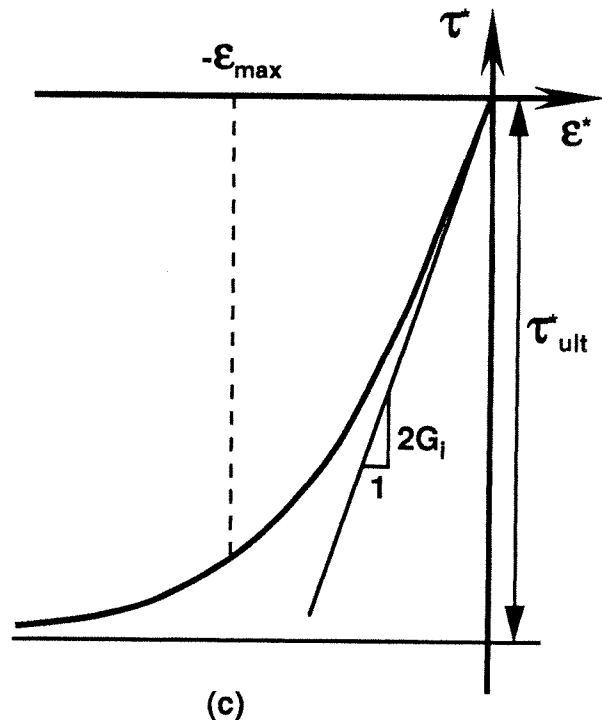
- Figure 1 - Proposed hyperbolic model for loading and unloading stages of a pressuremeter test; (a) loading and unloading; (b) loading part; (c) unloading part.
- Figure 2 - Interpretation methodology for a self-boring pressuremeter test (SBPT).
- Figure 3 - Interpretation methodology applied to: (a) Pre-bored pressuremeter tests (PMT) and (b) Full-displacement pressuremeter tests (FDPT).
- Figure 4 - Proposed template for interpreting pressuremeter data.
- Figure 5 - Interpretation of test V2P14 showing two typical plots: (a) suggested fit to last section of loading curve and (b) fit to all loading points.
- Figure 6 - Interpretation of test V2P10 showing the suggested fit to last section of loading curve.
- Figure 7 - Shear modulus versus depth, Fucino Clay.
- Figure 8 - Undrained shear strength versus depth, Fucino Clay.
- Figure 9 - Earth pressure coefficient at rest versus depth, Fucino Clay
- Figure 10 - Sensitivity to undrained shear strength, Fucino Clay - Test V2P14.
- Figure 11 - Sensitivity to shear modulus, Fucino Clay - Test V2P14.
- Figure 12 - Sensitivity to in-situ horizontal stress, Fucino Clay - Test V2P14.



(a)



(b)



(c)

FIGURE 1

Hyperbolic model for loading and unloading stages of a pressuremeter test: (a) Loading and unloading together; (b) Loading part; (c) Unloading part.

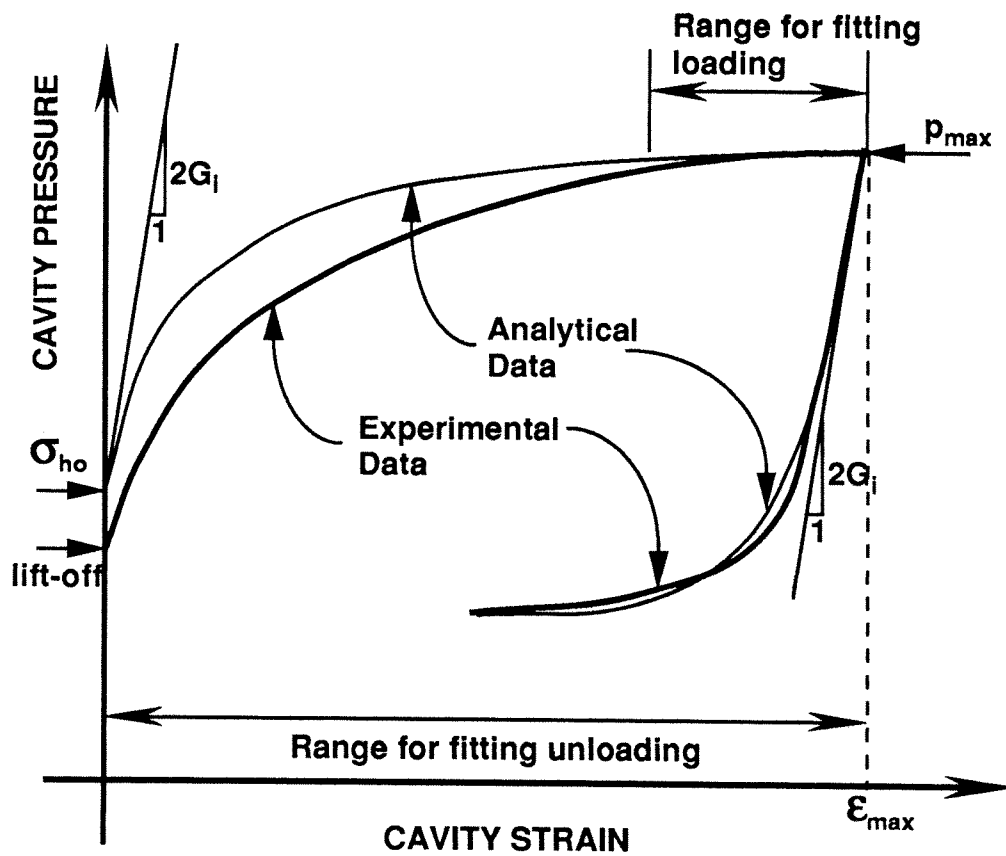
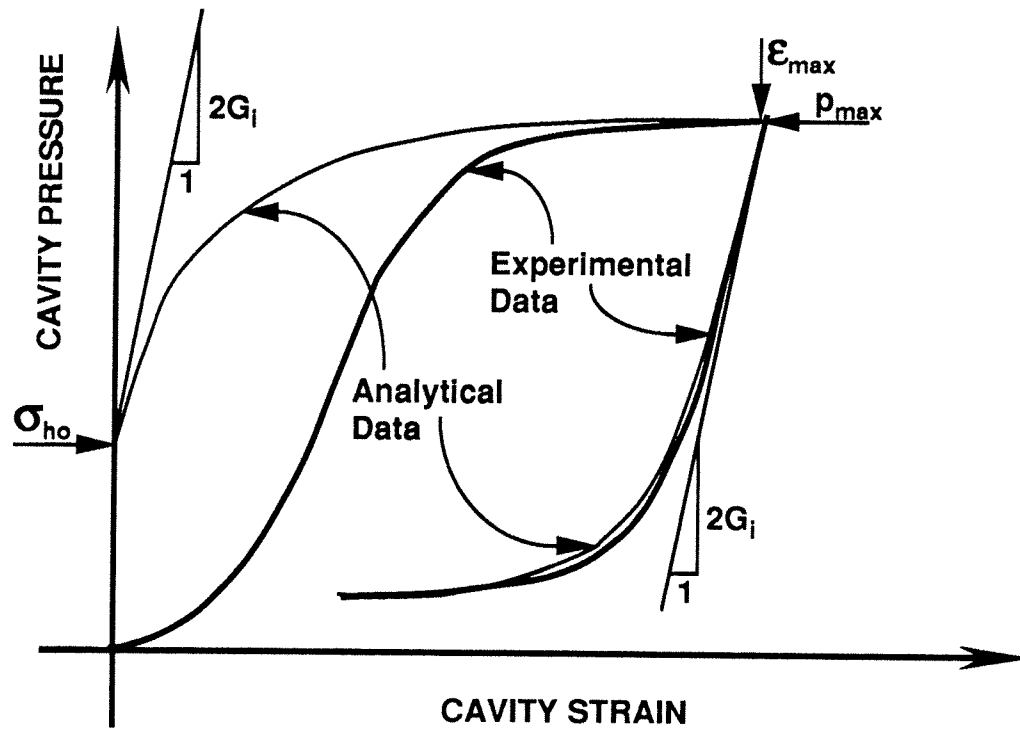
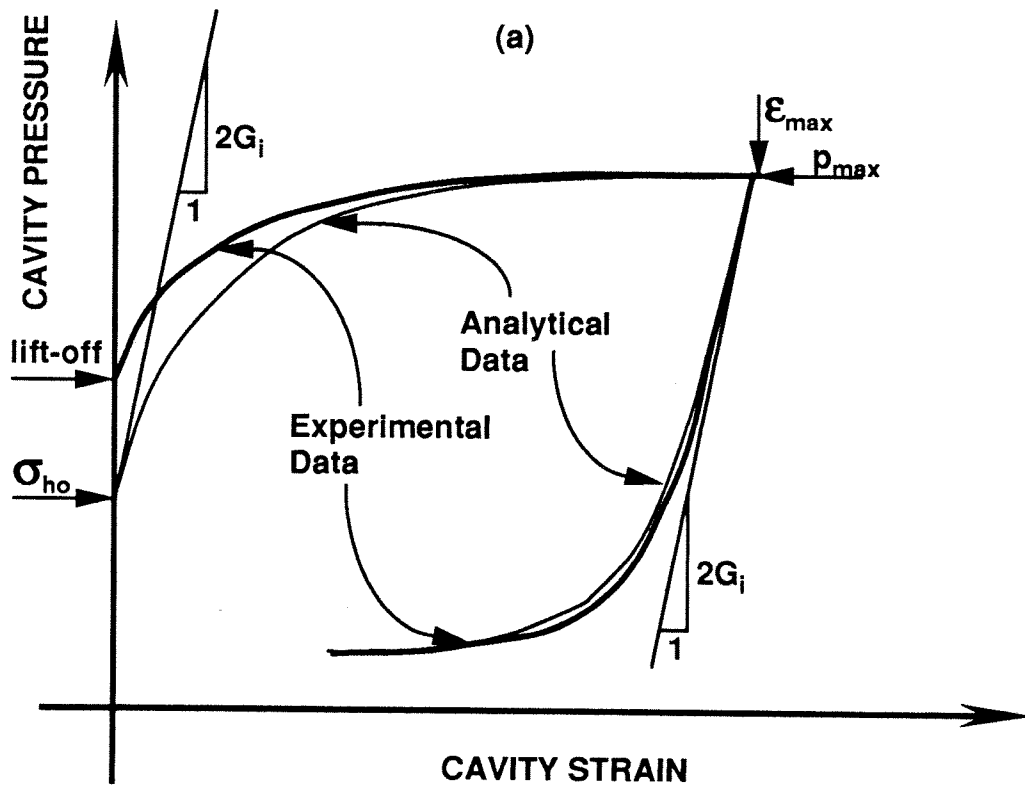


FIGURE 2
 Interpretation methodology for a self-boring pressuremeter test (SBPT).



(a)



(b)

FIGURE 3

Interpretation methodology applied to : (a) Pre-bored pressuremeter test (PMT); (b) Full-displacement pressuremeter test (FDPT).

PRESSUREMETER INTERPRETATION TEMPLATE

TEST ID	Fucino clay - Test V2P14		
DEPTH [m]	26.0	LIFT-OFF [kPa]	409.93
Loading : p_{\max} [kPa]	792.93	ϵ_{\max} [dec]	0.1025
Unloading : p_{\max} [kPa]	779.93	ϵ_{\max} [dec]	0.1074

STEP # 1 - UNLOADING (Best fit with two parameters)

(a) All unloading points

$\tau_{ult}^* = 233.0$
 $2G_1 = 22377.0$
 Graph Page Figures 5 (a) and (b)

(b) (some data points removed)

$\tau_{ult}^* =$
 $2G_1 =$
 Graph Page _____

STEP # 2 - LOADING (Best fit with one parameter $R_{\tau}=2.0$)

(a) All loading points

$\sigma_{ho} = 441.9$
 Graph Page Figure 5(b)

(b) Strain range (first option) Last half

$\sigma_{ho} = 444.4$
 Graph Page not shown

(c) Strain range (second option) Last quarter

$\sigma_{ho} = 443.0$
 Graph Page not shown

(d) Strain range (third option) Interpolate points at the very last end

$\sigma_{ho} = 441.7$
 Graph Page Figure 5(a)

STEP # 3 - SUMMARY

(a) First strain range selected Very last end

$\tau_{ult}^* = 233.0$ $\tau_{ult} = 116.5$
 $2G_1 = 22377.0$ $\sigma_{ho} = 441.7$
 Graph Page Figure 5 (a)

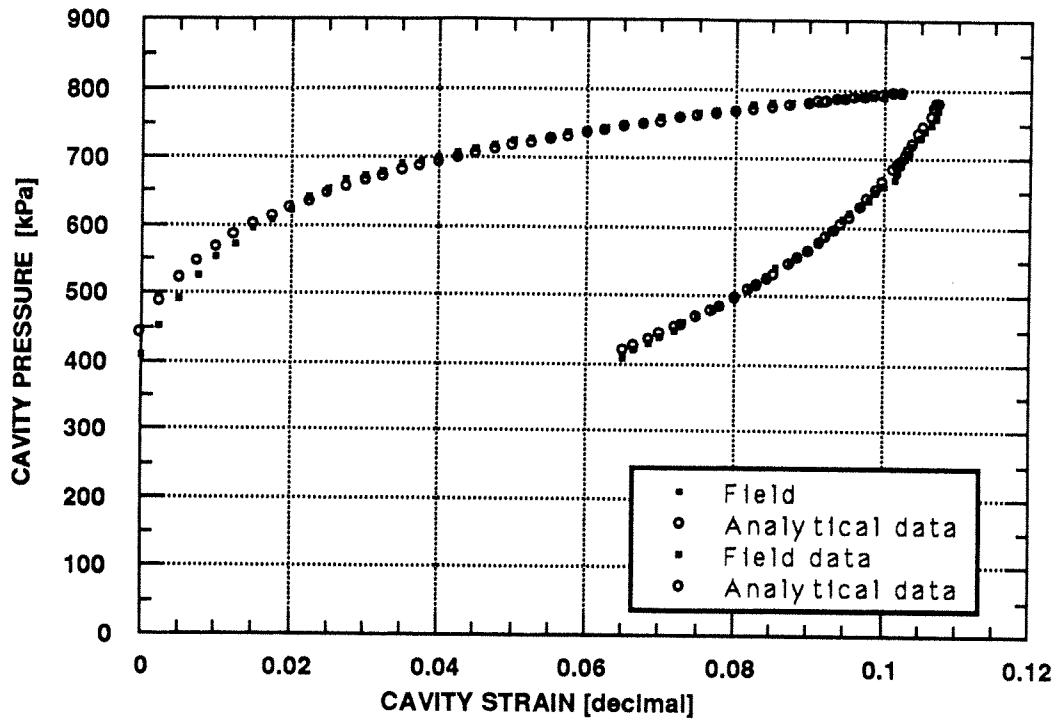
(b) Second strain range selected

$\tau_{ult}^* =$ $\tau_{ult} =$
 $2G_1 =$ $\sigma_{ho} =$
 Graph Page _____

FIGURE 4

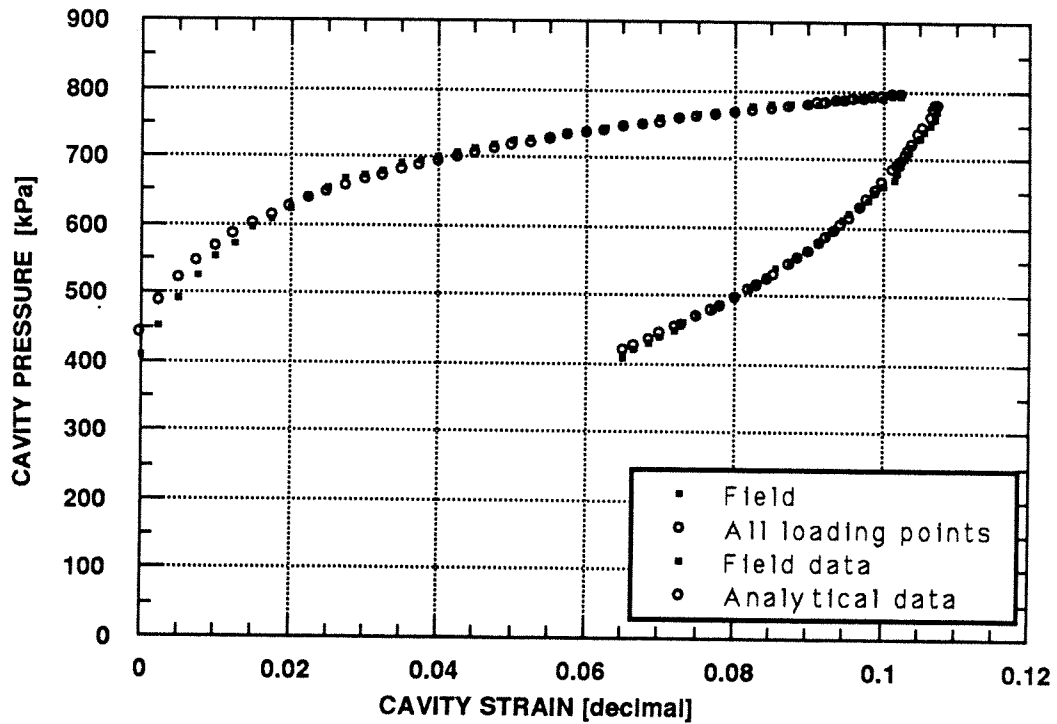
Template for interpreting pressuremeter data.

FUCINO CLAY - TEST V2P14 - FINAL PLOT



(a)

FUCINO CLAY - TEST V2P14 - FITTING ALL LOADING POINTS



(b)

FIGURE 5

Interpretation of test V2P14 showing two typical graphs: (a) Final plot; (b) Fitting all loading points.

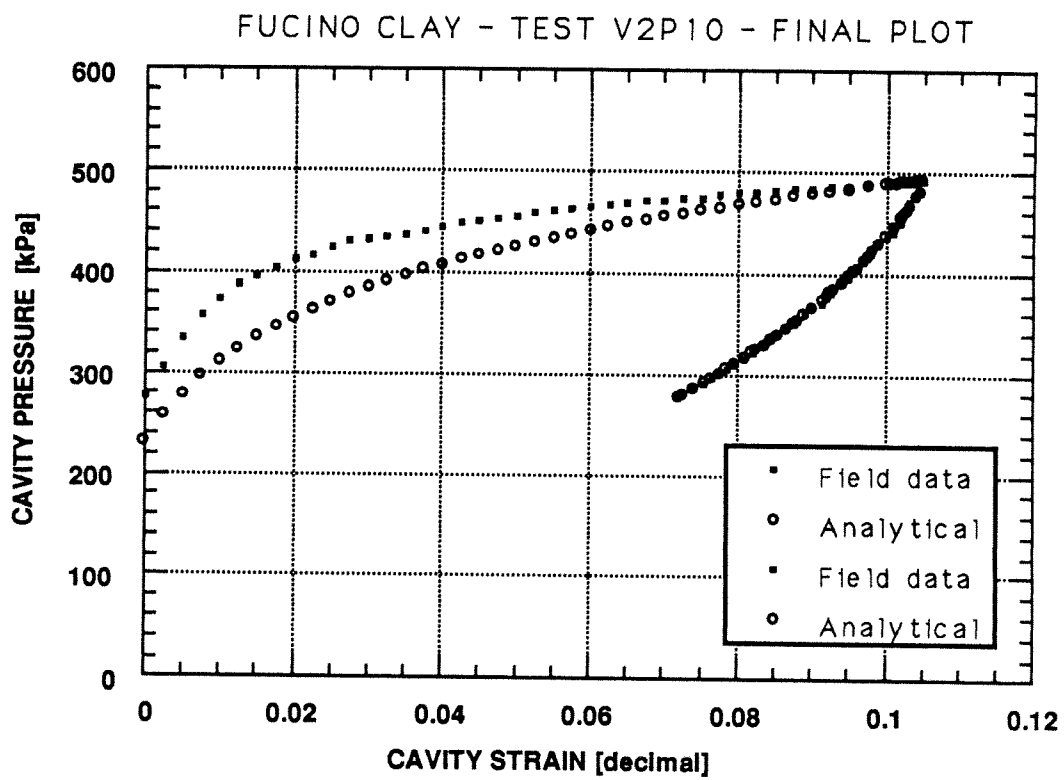


FIGURE 6

Interpretation of test V2P10 showing the final plot.

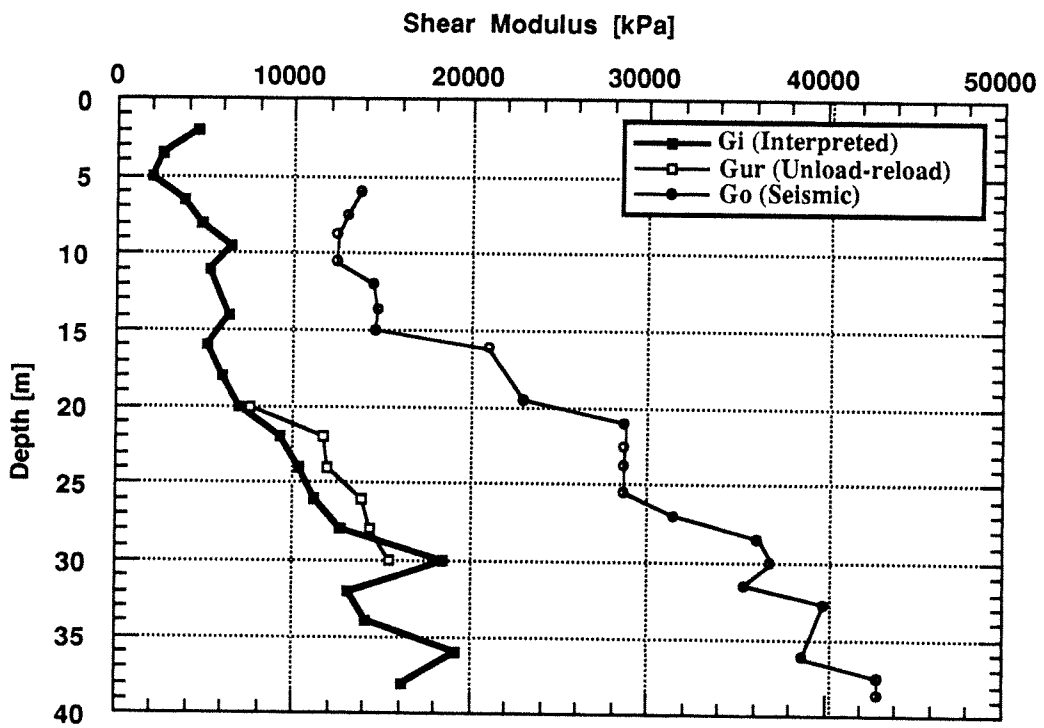


FIGURE 7

Undrained shear modulus versus depth, Fucino clay.

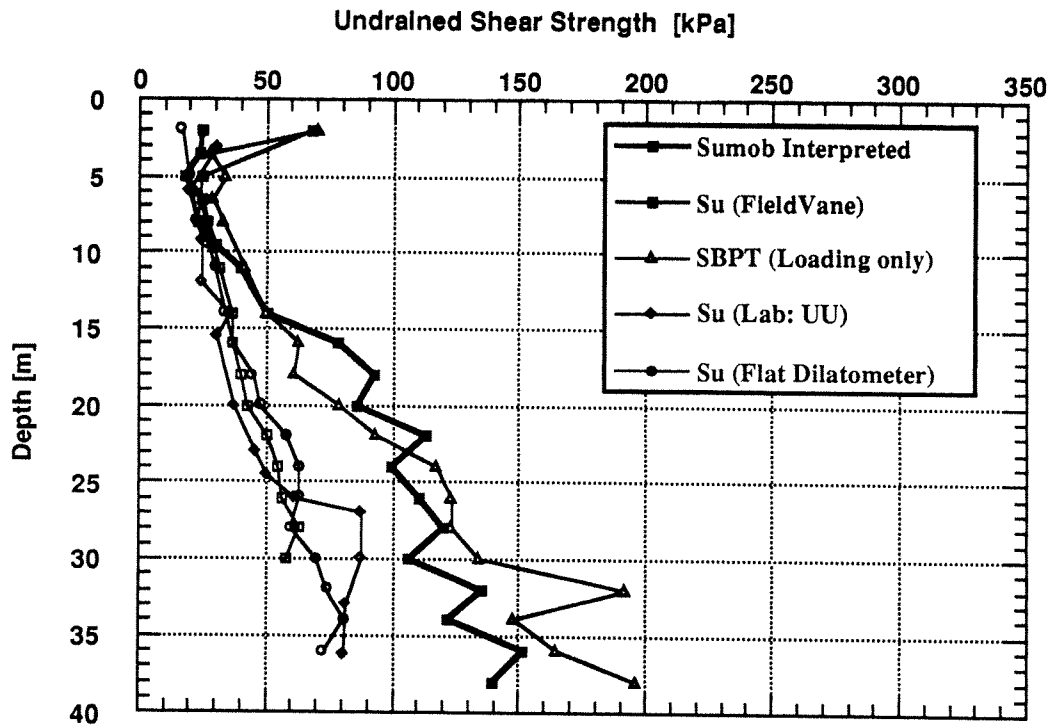


FIGURE 8

Undrained shear strength versus depth, Fucino clay.

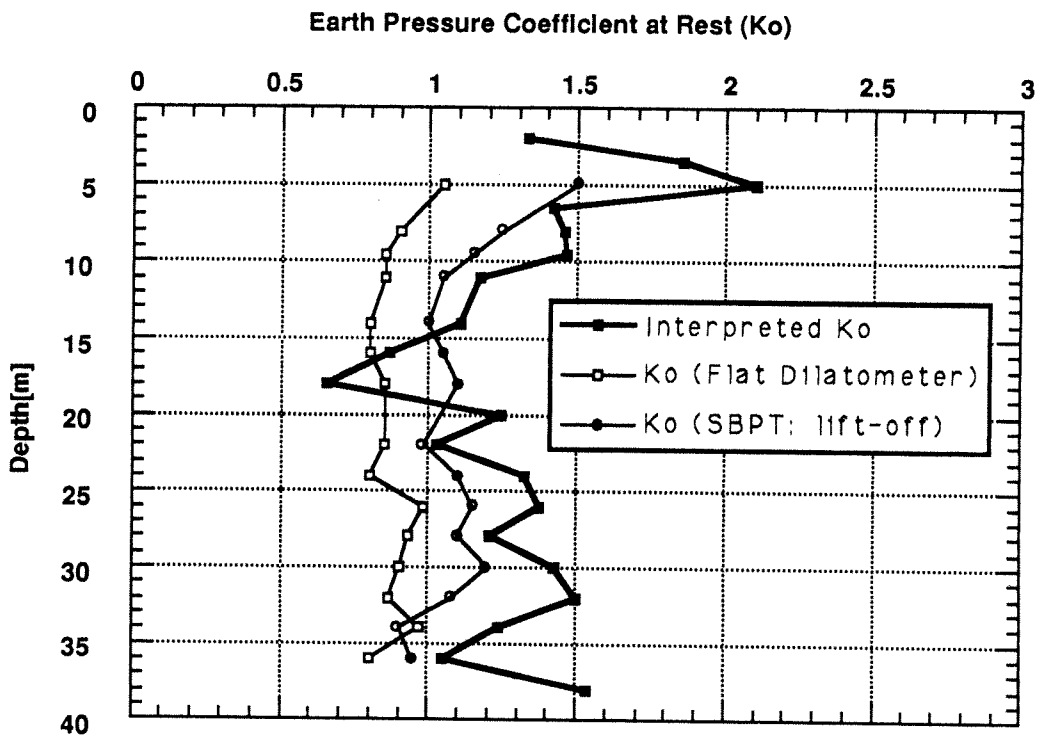


FIGURE 9

Earth pressure coefficient at rest versus depth, Fucino clay.

FUCINO CLAY - TEST V2P14 - SENSITIVITY TO
UNDRAINED SHEAR STRENGTH

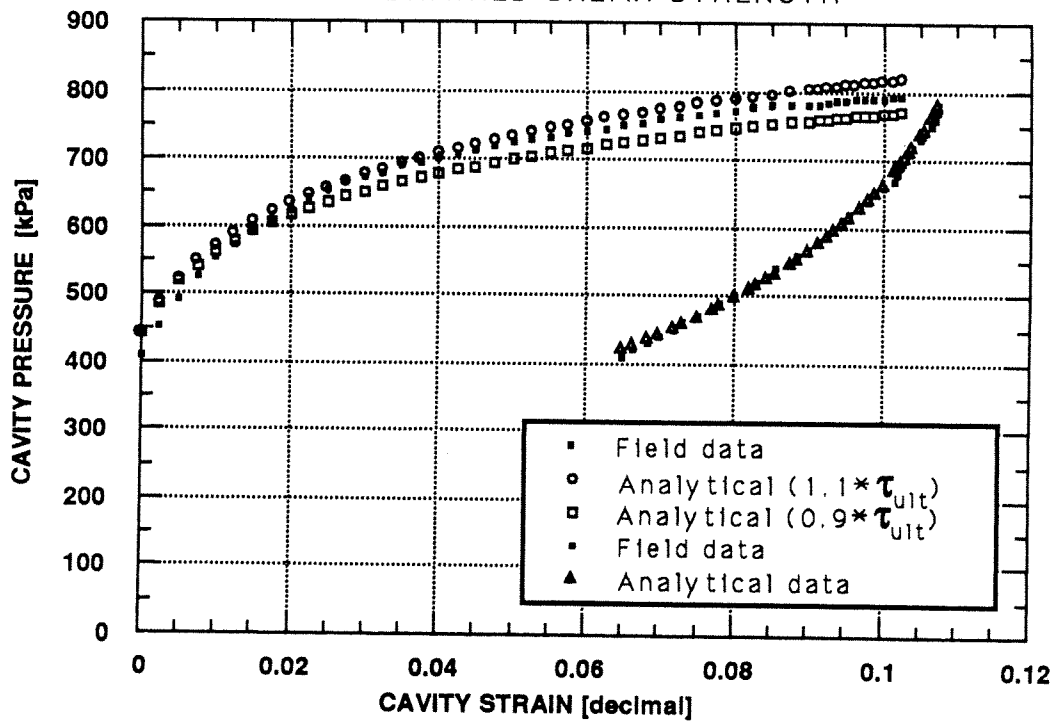


FIGURE 10

Fucino clay - Test V2P14 - Sensitivity to undrained shear strength.

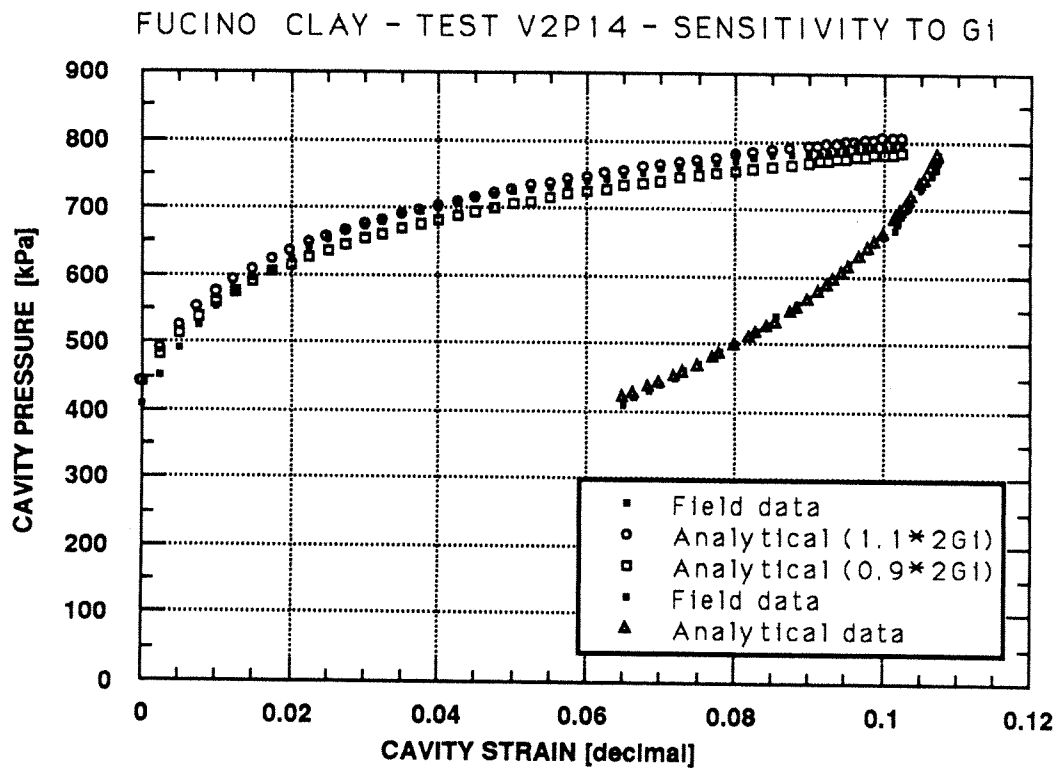


FIGURE 11

Fucino clay - Test V2P14 - Sensitivity to shear modulus.

FUCINO CLAY - TEST V2P14 - SENSITIVITY TO INITIAL HORIZONTAL STRESS

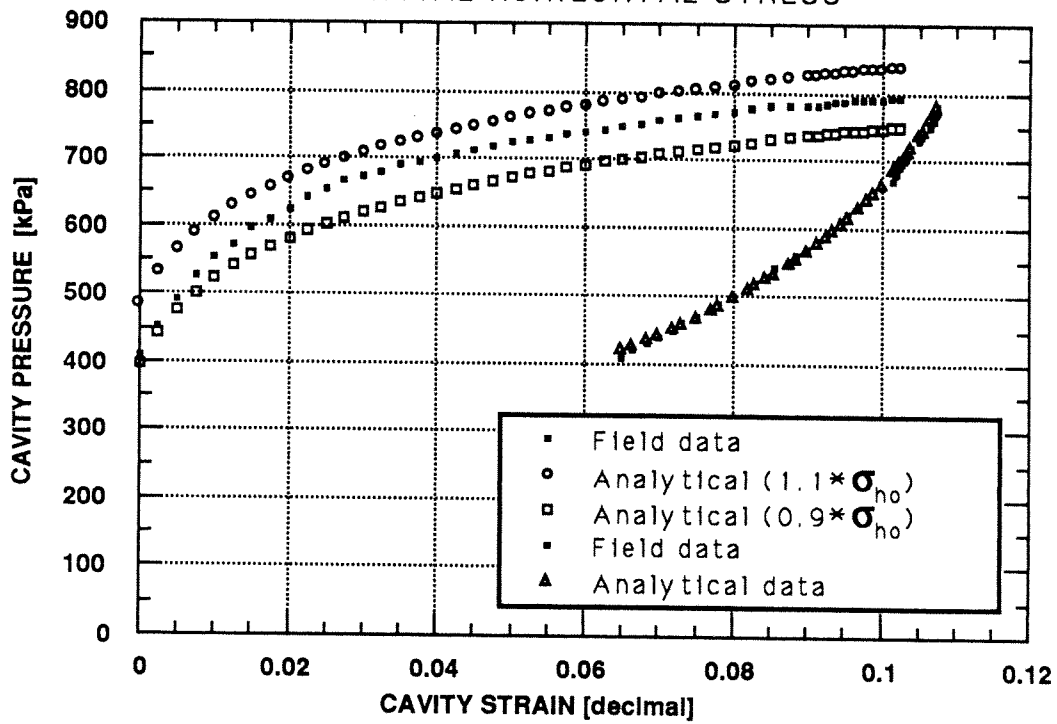


FIGURE 12

Fucino clay - Test V2P14 - Sensitivity to initial horizontal stress